Profiling of EV-containing SEC fractions with single-molecule imaging

SUMMARY

Investigating the biomarker distribution and size of Extracellular Vesicles (EVs) purified using Size Exclusion Chromatography (SEC) enhances our understanding of how the EV purification method influences output EV population numbers, EV integrity and morphology, and the investigation of EV biomarker content.

The Nanoimager and ONI Application Kit: EV Profiler 2™ enable:

- Quantification of EVs and their biomarkers, with 20 nm resolution
- EV sizing and morphological identification using a generic Pan-EV stain
- Simultaneous EV sizing and detection of custom biomarkers of interest
- Detection of cargo molecules contained inside EVs using permeabilization

INTRODUCTION

Cell-to-cell communication allows cells to coordinate development and send crucial signals regarding cell environment and health. Extracellular vesicles (EVs) are lipid bilayer-bound particles that range in size and that play critical roles in cell-cell communication to maintain tissue homeostasis and as carriers of disease state markers, including RNA/DNA, cytosolic or membrane-bound proteins, and other signaling factors[1,2]. EVs have gathered special interest in the last few years through their potential as vehicles for drug-based cell targeting, vaccine delivery, and biomarkers of various diseases, including cancers and viral infections[3-5].

EVs appear to be released by all cell types and can be found in most biofluids such as milk, plasma, urine, semen, and cerebrospinal fluid[6]. They can also be found in conditioned cell culture media. However, most techniques currently available for EV characterization require the use of purified samples, where EVs have been separated from potential contaminants such as soluble proteins and non-EV lipid particles. A variety of EV purification methods have been developed over the years, the most common methods include: ultracentrifugation (UC), polymer-based precipitation, size exclusion chromatography (SEC) and density-gradient centrifugation[7]. Each method has different benefits and limitations, depending on the EV source and the downstream technique to be used to analyze purified EVs. Here, we will focus on SEC and how ONI's EV Profiler 2 kit can be used to characterize the different fractions that are isolated using SEC. For more information about EV purification methods compatible with single-molecule imaging using the Nanoimager, please refer to ONI's webinar entitled "Preparing intact EV samples for super-resolution imaging".

METHODS

PANC1 cells were cultured in phenol red-free Dulbecco's Modified Eagle's Medium (DMEM) supplemented with 10% EV-depleted FBS and 1% penicillin/streptomycin (Gibco™ 21063045, A2720803 and 15140122). Conditioned medium was collected after 48 hours for EV isolation and spun at 300 x g for 10 minutes to remove cellular debris. Clarified conditioned medium was concentrated to 400 µL using Vivaspin™ 20 100kDa concentrators (Cytiva 28932363) at 1000 x g in 10-minute intervals. Concentrated medium was loaded into IZON qEVoriginal Gen 2 70 nm column (IZON ICO-70) equilibrated at room temperature with ONI's Wash Buffer according to the manufacturer's instructions. SEC collection was performed manually, using gravity flow. 2.75 mL of void volume was discarded, then 125 µL subfractions (fraction 6b, 7a, 7b, 7c, 7d, and 8a, respectively) were collected off the qEVoriginal column. Collected subfractions were used for subsequent preparation using ONI's Application Kit: EV Profiler 2. All subfractions were diluted 1:5 in Wash Buffer before being applied to the EV Assay Chip. EVs were captured using phosphatidylserine (PS) Capture, and detected using both the Tetraspanin profiling and the Pan-EV detection modalities. Imaging was performed on a Nanoimager Mark II S using NimOS, and analysis was performed using ONI's CODI, using the "EV Profiling" analysis app with the DBscan algorithm used to cluster localization data. Data were plotted using Graphpad Prism 10.2.2.

RESULTS

PANC1 EVs were isolated and purified using IZON's SEC-based qEV 70 nm columns, whereby samples can be collected in 500 µL fractions, and the first 3 mL or 6 fractions considered the void volume containing soluble proteins and non-EV lipid particles. Here, we captured the final 250 µL of fraction 6 (termed subfraction 6b) and subdivided the 7th fraction into four 125 µL subfractions (7a, 7b, 7c, 7d, respectively), as well as collecting the first 250 µL sub-fraction of fraction 8 (subfraction 8a). Purified EVs were then captured using ONI's EV Profiler 2 PS capture so as not to bias the EV capture only to those with tetraspanins. Total EV counts were calculated using CODI's "EV Profiling" analysis app with DBSCAN clustering of the Pan-EV detection modality.

The amount of EVs collected and captured onto the assay surface decreased with each subfraction, as expected (Figure 1). While a large number of EV-like particles captured from subfraction 6b were observed, there was high variability in the number of EVs captured across 8 FOVs. In alignment with the manufacturer's instructions to discard this fraction, there is a higher likelihood of contamination (e.g., lipoproteins that are similar in size to EVs) in fraction 6 despite EV-like particles being captured from this fraction.

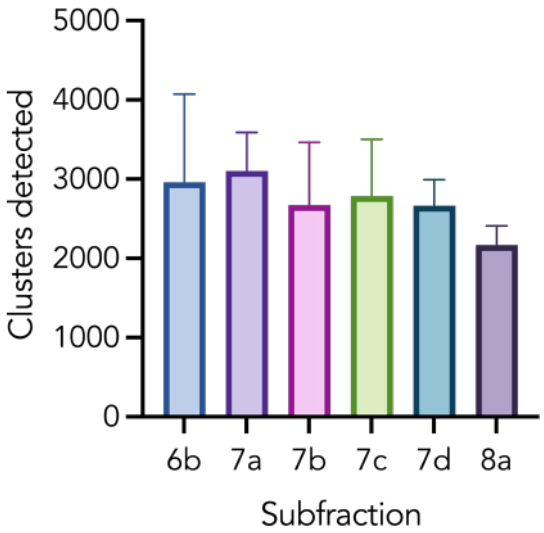

Figure 1 | The number of EVs purified decreases with each subfraction. EVs detected via DBscan clustering using the Pan-EV Detection modality. Mean of 8 FOVs with SD shown.

Due to the principles of SEC, larger EVs are expected to exit the column first. Indeed, using ONI's Pan-EV stain, we can observe that the diameter of EVs captured onto the Assay Chip decreases throughout subfraction collection. The EV populations collected from subfractions 6b, 7b, and 7c had a median diameter of approximately 120-140 nm, while EVs from subfractions 7d and 8a had a median diameter of 101 nm and 94 nm, respectively (Figure 2). Notably, the range of EV diameters present in each subfraction also shifted to the left throughout the SEC fractions, matching the decrease observed in the fractions' median diameter (Figure 2 top and bottom, respectively).

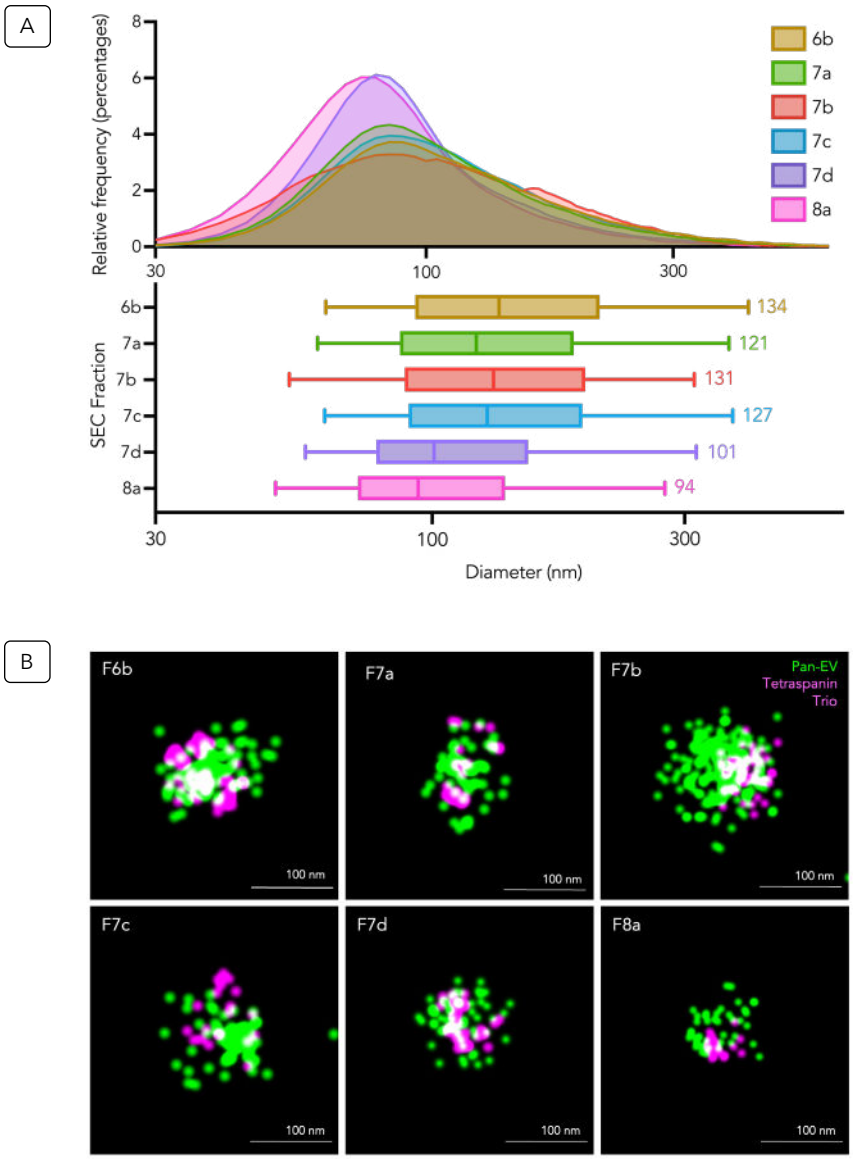

Figure 2 | EV diameter decreases with each subfraction. A) Top: Relative frequency distribution histogram of EV sizes within each subfraction. The X-axis is a log10 scale. A bin size of 5 nm was used for the histogram, and the resultant histogram was smoothed using second-order smoothing of 9 neighbors. A) Bottom: Box and whiskers plot showing each EV SEC fraction diameter distribution, whereby the median value has been annotated. Note: A cluster size of 30 nm is the minimum defined by CODI, to provide high confidence in EV identity. B) Representative single-EV images from each EV subfraction collected using SEC and labeled with Pan-EV stain (green) and tetraspanin-trio (magenta) to confirm EV identity and assess morphology. EVs were imaged with super-resolution imaging on ONI's Nanoimager and localization data processed with cluster-based analysis using the "EV Profiling" analysis app on CODI.

While we were able to investigate EV size and approximate sample concentration using the Pan-EV detection modality of the EV Profiler 2 kit, we can also use the Tetraspanin Profiling detection modality to investigate how the tetraspanin content of these EVs changes among the different purification fractions. In this case, we observed minimal differences in CD81, CD63, and CD9 content between the subfractions collected and imaged. No clear trends were observed in tetraspanin (CD9, CD63, and CD81) content between the subfractions (Figure 3).

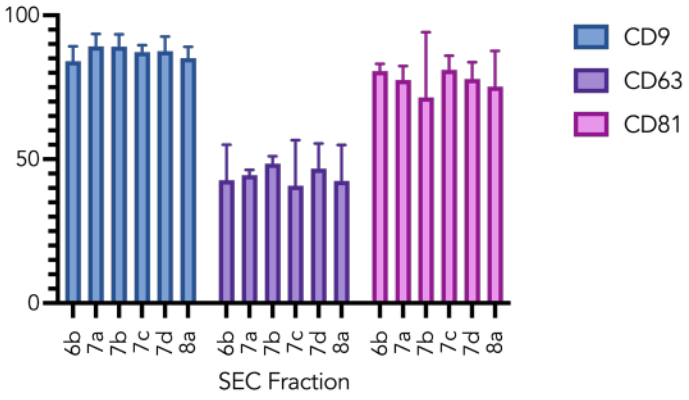

Figure 3 | Minimal changes in tetraspanin content occur from fraction 6a to 8a. Percentage of clusters positive for CD81, CD63, and CD9 respectively. Each FOV was normalized to total clusters in the FOV. Mean with SD shown.

CONCLUSIONS

Here, we demonstrate how to use both ONI's EV Profiler 2 kit Tetraspanin Profiling and Pan-EV detection modalities, together with the Nanoimager microscope and CODI software tools, to characterize an EV population and compare between different purified EV populations. Enabling investigation of EV size and EV protein content via single-molecule imaging will allow EV researchers to better understand their EV populations at a single EV level and delve into heterogeneity within a population. In turn, this will enable a better understanding of EV biology and how EVs can be used for diagnostics, discovery, and drug delivery.

REFERENCES

1. Dixson AC, Dawson TR, Di Vizio D. et al. Context-specific regulation of extracellular vesicle biogenesis and cargo selection. Nat Rev Mol Cell Biol 24, 454–476 (2023). https://doi.org/10.1038/s41580-023-00576-0

2. Yates AG, Pink RC, Erdbrügger U. et al. In sickness and in health: The functional role of extracellular vesicles in physiology and pathology in vivo: Part I: Health and Normal Physiology: Part I: Health and Normal Physiology. J Extracell Vesicles. 11(1):e12151 (2022). https://doi.org/10.1002/jev2.12151

3. Kim J, Lee SK, Jeong SY. et al. Cargo proteins in extracellular vesicles: potential for novel therapeutics in non-alcoholic steatohepatitis. J Nanobiotechnol 19, 372 (2021). https://doi.org/10.1186/s12951-021-01120-y

4. Katsuda T, Kosaka N, Ochiya T, The roles of extracellular vesicles in cancer biology: Toward the development of novel cancer biomarkers. Proteomics 14, 412-425 (2014). https://doi.org/10.1002/pmic.201300389

5. Hurwitz SN, Rider MA, Bundy JL. et al. Proteomic profiling of NCI-60 extracellular vesicles uncovers common protein cargo and cancer type-specific biomarkers. Oncotarget. 7(52):86999-87015 (2016). https://doi.org/10.18632/oncotarget.13569

6. van Niel G, D'Angelo G & Raposo G. Shedding light on the cell biology of extracellular vesicles. Nat Rev Mol Cell Biol 19, 213–228 (2018). https://doi.org/10.1038/nrm.2017.125

7. Brennan K, Martin K, FitzGerald SP et al. A comparison of methods for the isolation and separation of extracellular vesicles from protein and lipid particles in human serum. Sci Rep 10, 1039 (2020). https://doi.org/10.1038/s41598-020-57497-7